Supplementary Information for

A decline in atmospheric CO_2 levels under negative emissions may enhance carbon retention in the terrestrial biosphere

So-Won Park[1] and Jong-Seong Kug[1*]

[1]Division of Environmental Science and Engineering,

Pohang University of Science and Technology (POSTECH), Pohang, South Korea

*Corresponding author. Email: jskug@postech.ac.kr

Supplementary Note 1: Uncertainty in the projection of terrestrial C cycle in Amazonia

The land C stock in Amazon at 2×CO_2 and 1×CO_2 between the ramp-down and -up period varies among ESMs, indicating a high degree of uncertainty in future changes in the terrestrial C cycle in Amazon (Fig. 3 and Supplementary Fig. 6). To understand the different terrestrial ecosystem responses to CO_2 forcing in Amazon, we divided the models into two groups, depending on the discrepancy in the total land C stock anomaly at 2×CO_2 (positive: group A; negative: group B) and conducted a composite analysis (Supplementary Fig. 7). In group B models, the annual mean temperature increase to CO_2 forcing is greater, up to 2.5 K, than that of group A. In addition, group A models show a feeble change in precipitation in the CO_2 ramp-up period, whereas ESMs in group B simulate the decrease in precipitation in Amazon. These changes in climate conditions in group B considerably decrease the vegetation productivity. Consequently, in group B, the land is converted to a C source at the CO_2 peak without a delayed response due to the low productivity, and the total land C stock rapidly decreases, leading to an overshoot of about ~13 Gt C in Amazon at the end of the experiment. These results imply that precipitation change is very important for the vegetation growth and hence land C stock in Amazonia. However, the highly uncertain precipitation change in tropical land still remains a problem[1].

Supplementary Note 2: The simulation of permafrost carbon and process in CESM2 and NorESM2-LM

The Community Land Model 5 (CLM5) has improved its components, such as snow density and insulation, soil layer resolution, and soil hydrology in the cold region, to simulate more realistic permafrost distribution, active layer dynamics, and hydrology[2]. The CLM5, land surface model (LSM) in CSEM2 and NorESM2-LM, includes the dynamics of deep and frozen soil carbon and hence permafrost carbon, while the other LSMs simulate the soil biogeochemistry only using the near-surface soil temperature. Therefore, only CESM2 and NorESM2-LM coupled with CLM5 are suitable for the examination of permafrost carbon feedbacks to climate change. In addition, CESM2 and NorESM2 were assessed to have good skills in simulating the permafrost extent, the effective snow depth, which describes the insulation of snow over the cold period, and the annual mean frozen volume[3]. However, there are still uncertainties and problems in simulating the permafrost processes due to biases in simulated surface climate and LSM and the problem about initialization[3,4]. First, the model initialization process for soil carbon is artificial, and thus the soil carbon in the high Arctic grid cell is somewhat high compared to the field-based soil carbon estimate from NCSCDv2[5] (Supplementary Fig. 9). Second, there is warm bias in CESM2 and NorESM2-LM, thereby causing the overestimation of annual mean thawed volume. Third, the biases in snow amount and physics would influence the snow insulation and thus result in the uncertainties of permafrost carbon pool. Therefore, at the current stage, our results include the uncertainties from both these model's biases and the flaw of simulation.

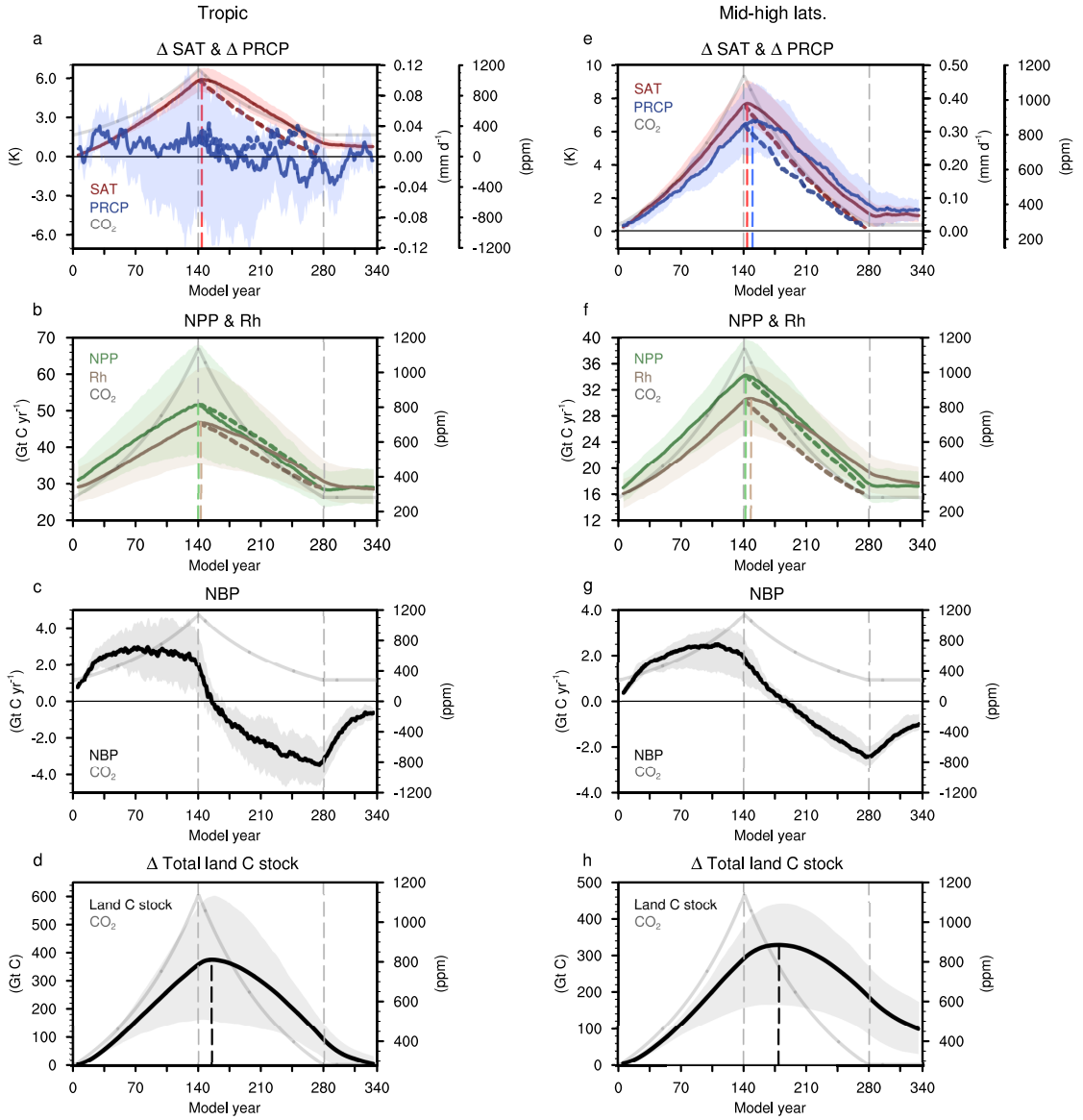

Supplementary Fig. 1 | Temporal evolution of terrestrial carbon fluxes and stock in tropic and mid-high latitudes. a–h, Time-series of annual mean land surface air temperature (SAT) and precipitation (PRCP) anomaly **(a,e)**, annual net primary production (NPP) and heterotrophic respiration (Rh) **(b,f)**, annual net biome productivity (NBP) **(c,g)**, and annual mean total land C stock anomaly **(d,h)** in tropic **(a-d)** and mid-high latitude **(e-h)** in an idealized CO_2 ramp-up and -down experiment. The solid lines and shadings show the MME mean and range of 95% confidence level based on the bootstrap method. Colored dash lines show the response to CO_2 ramp-up forcing vertically mirrored about 140 model year to represent the asymmetry in the responses. All values are smoothed by the 11-year moving average. The gray solid lines represent the atmospheric CO_2 concentration, and the beginning and end of CO_2 changes are indicated by the gray dashed vertical line.

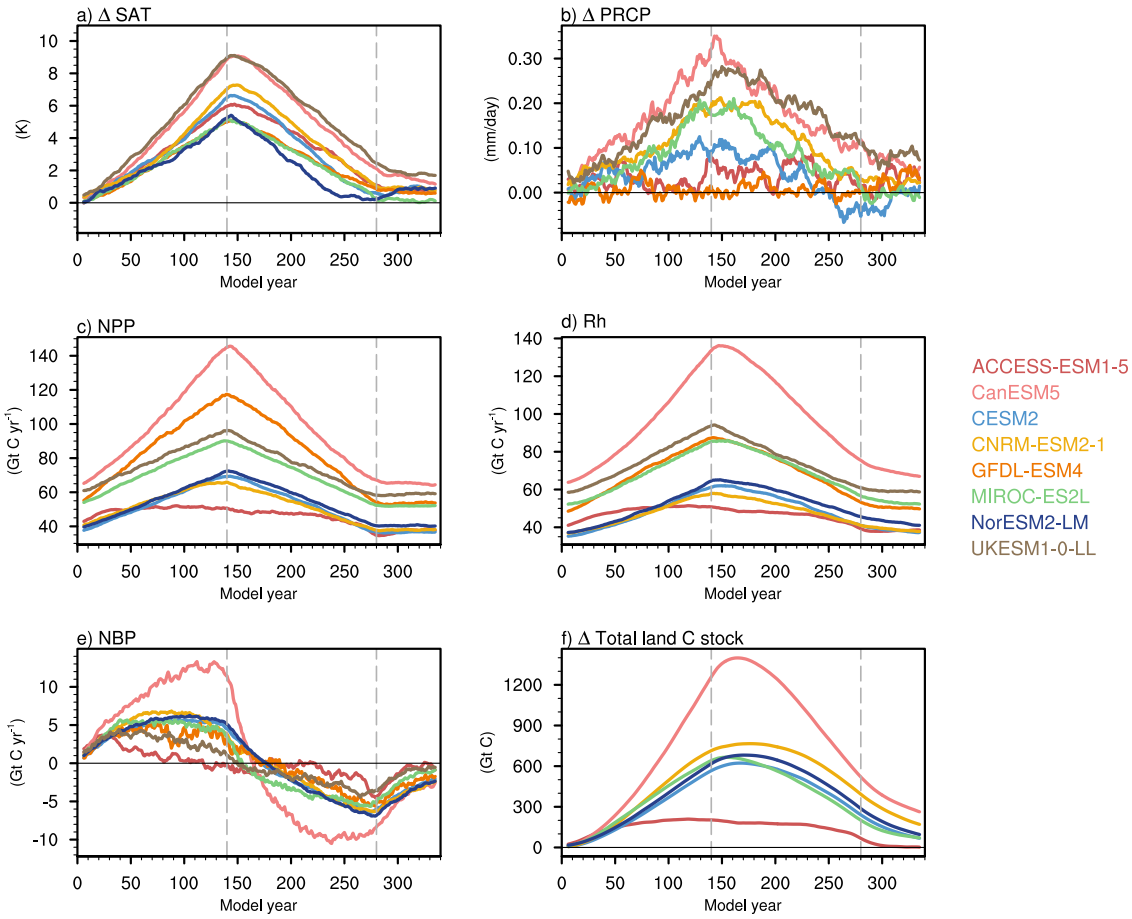

Supplementary Fig. 2 | Intermodel diversity of temporal evolution of global land carbon fluxes and stock. a–f, Time-series of global annual mean land SAT **(a)** and PRCP **(b)** anomaly, annual NPP **(c)**, annual Rh **(d)**, annual NBP **(e)**, and annual mean total land C stock anomaly **(f)** from CMIP6 ESMs. All values are smoothed by the 11-year moving average. The beginning and end of CO_2 changes are indicated with the gray dashed vertical line.

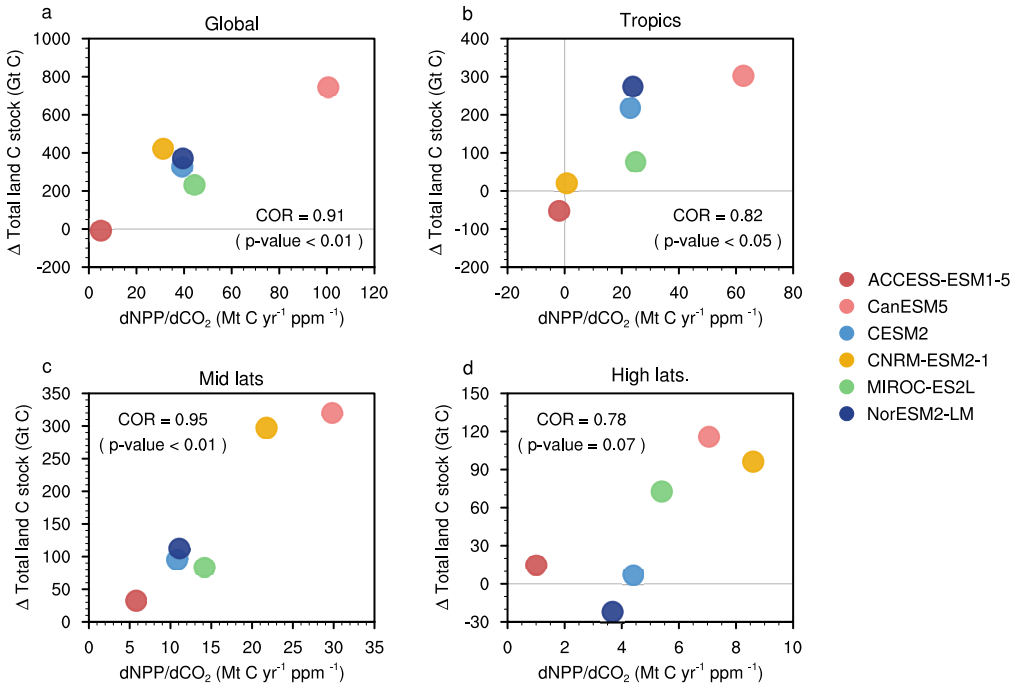

Supplementary Fig. 3 | Inter-model diversity of lagged response of terrestrial carbon cycle. **a-d,** Scatterplots of the average rate of NPP change to ramp-up CO_2 forcing versus the difference of the total land C stock anomaly between model Year 210 and 70 averaged over the whole globe **(a)**, tropic (30°S–30°N) **(b)**, mid-latitudes (30°–60°N) **(c)**, and high-latitudes (above 60°N) **(d)**. All calculations were conducted after taking the 11-year moving average.

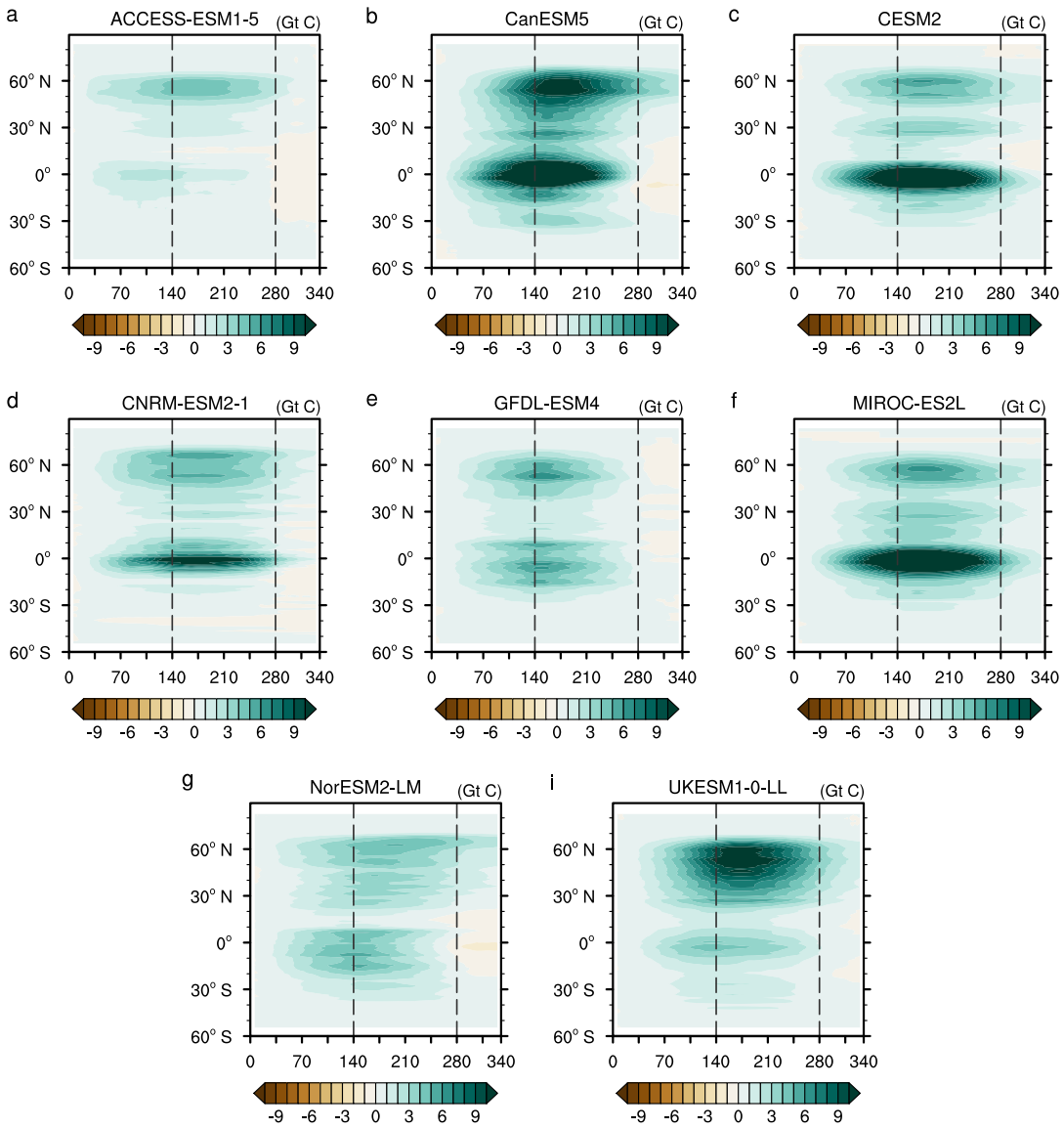

Supplementary Fig. 4 | Latitudinal differences in the response of terrestrial vegetation carbon (cVeg) anomaly to CO_2 ramp-up and -down forcing. a–i, Time-latitude diagrams of the cVeg anomaly from eight CMIP6 ESMs. All values are annual mean and smoothed by the 11-year moving average. The beginning and end of CO_2 changes are marked with a gray dashed vertical line.

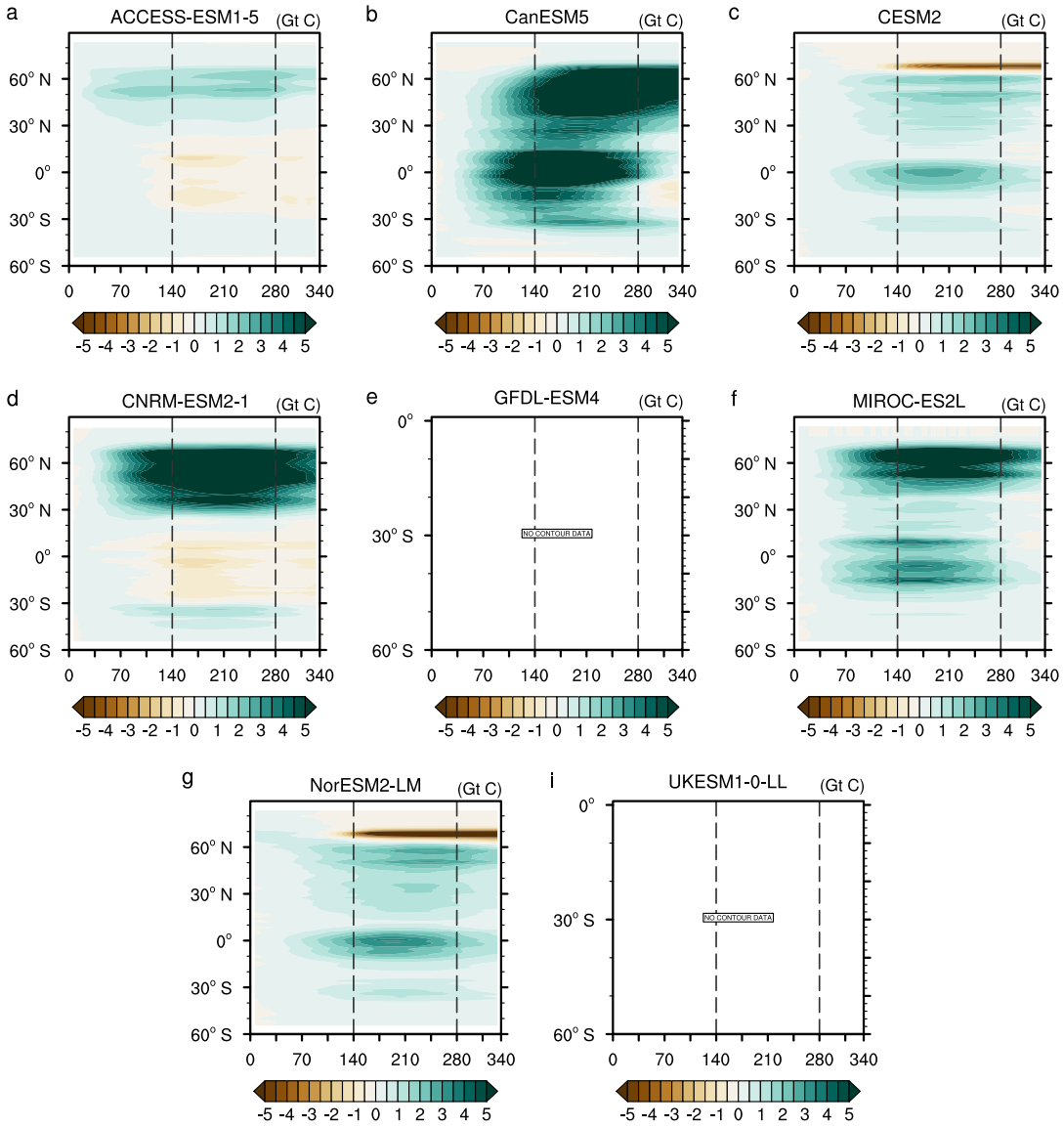

Supplementary Fig. 5 | Latitudinal differences in the response of terrestrial carbon anomaly in the litter-soil system to CO_2 ramp-up and -down forcing. a–i, Time-latitude diagrams of the sum of cLitter and cSoil anomaly from six CMIP6 ESMs. All values are the annual mean and smoothed by the 11-year moving average. The beginning and end of CO_2 changes are marked with the gray dashed vertical line. GFDL-ESM4M does not provide cLitter and cSoil data, and UKESM1-0-LL does not provide the cLitter data.

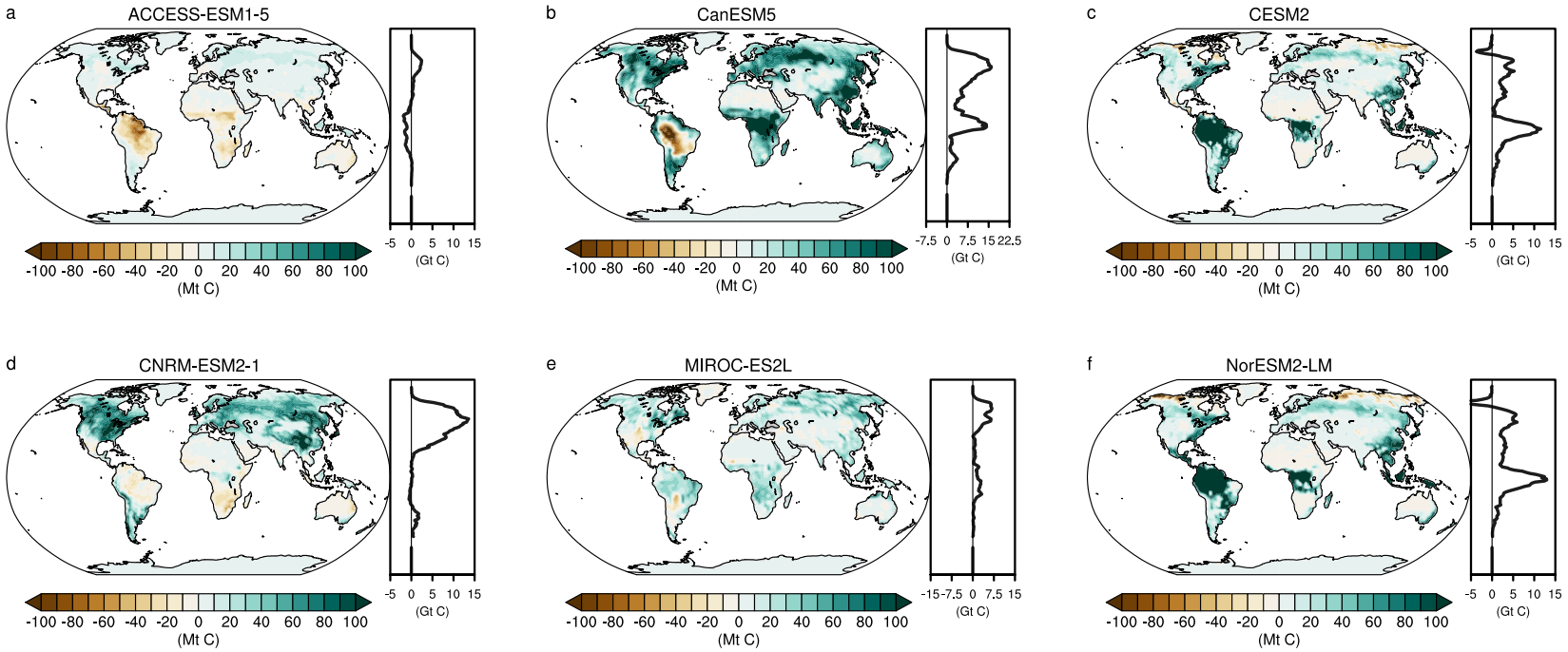

Supplementary Fig. 6 | Difference of total land carbon stock to CO_2 ramp-up and ramp-down forcing at a doubling of CO_2. a–f, Difference of total land C stock anomaly between model Year 210 and 70 ($2\times CO_2$) from six CMIP6 ESMs. All calculations were conducted after taking the 11-year running mean. GFDL-ESM4M does not provide cLitter and cSoil data and UKESM1-0-LL does not provide the cLitter data.

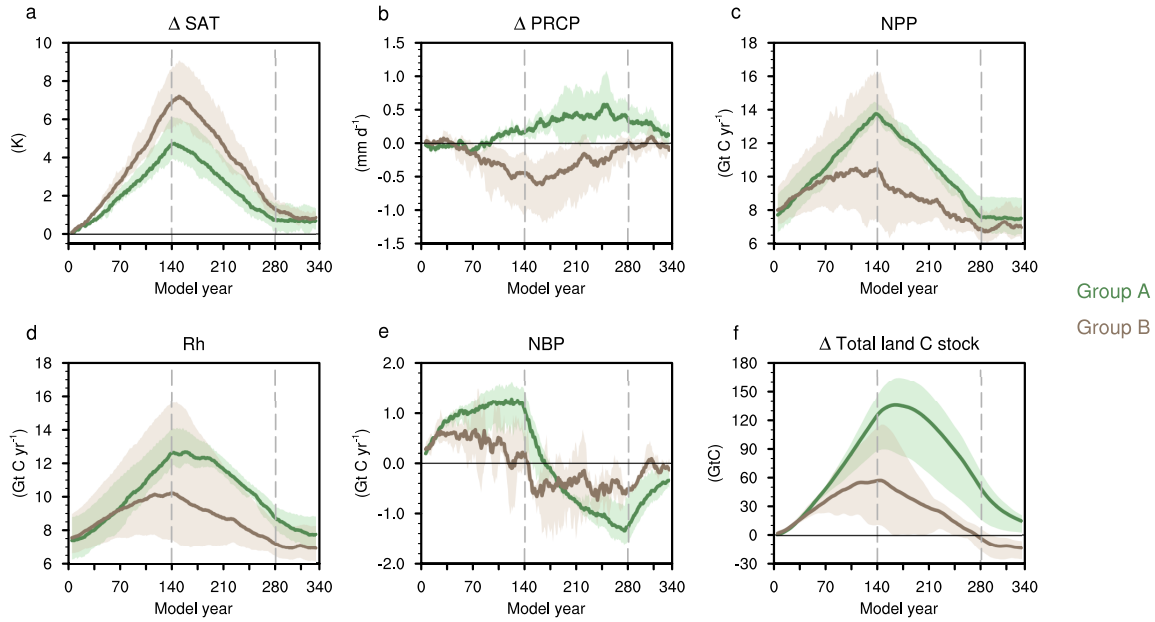

Supplementary Fig. 7 | Composite analysis of land carbon fluxes and stock in Amazon. a–f, Composite of time-series of annual mean land SAT **(a)** and PRCP **(b)** anomaly, annual NPP **(c)**, annual Rh **(d)**, annual NBP **(e)**, and annual mean total land carbon stock anomaly **(f)** in Amazon for group A models (CESM2, MIROC-ES2L, and NorESM2-LM) and group B models (ACCESS-ESM1-5, CanESM5, and CNRM-ESM2-1). The solid lines and shadings show the composite mean and range of 95% confidence level based on the bootstrap method. All values are smoothed by the 11-year moving average. The beginning and end of CO_2 changes are indicated by the gray dashed vertical line.

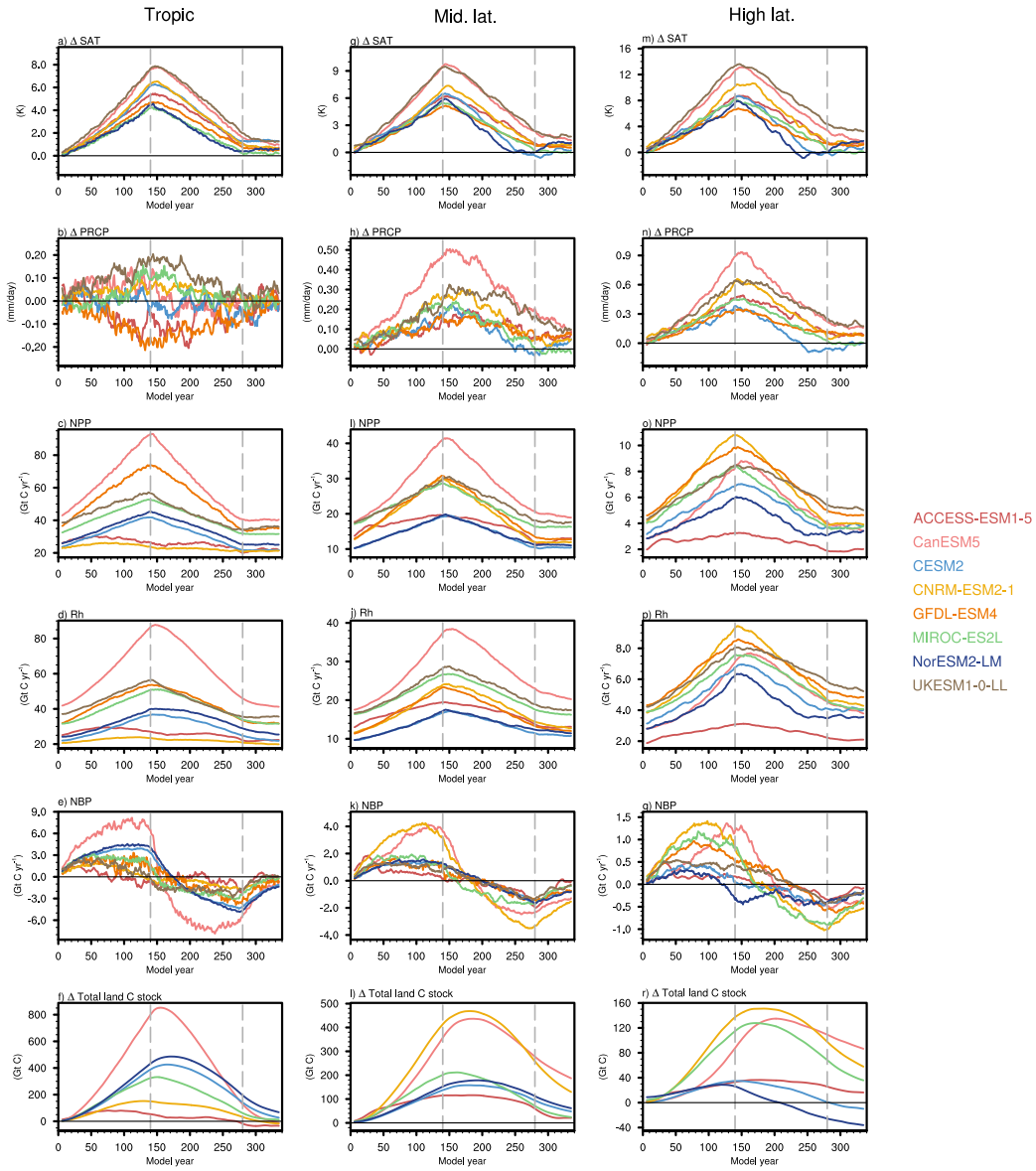

Supplementary Fig. 8 | Inter-model diversity of temporal evolution of land carbon fluxes and stock. a–r, Time-series of annual mean land SAT **(a, g, m)** and PRCP **(b, h, n)** anomaly, annual NPP **(c, i, o)**, annual Rh **(d, j, p)**, annual NBP **(e, k, q)**, and annual mean total land C stock anomaly **(f, l, r)** in tropic (30°S–30°N) **(a–f)**, mid-latitudes (30°–60°N) **(g–l)**, and high latitudes (above 60°N) **(m–r)** from CMIP6 ESMs. All values are smoothed by the 11-year moving average. The beginning and end of CO_2 changes are indicated with the gray dashed vertical line.

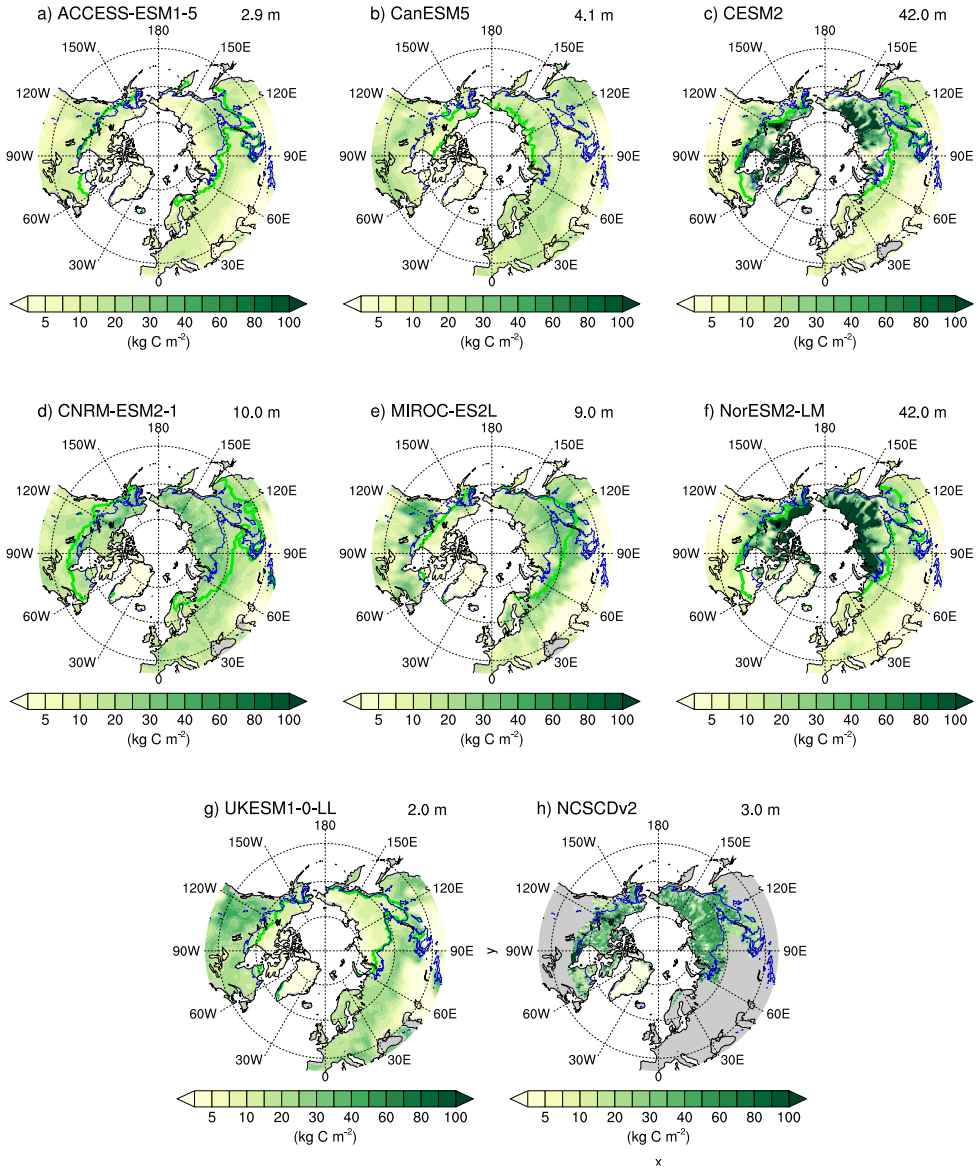

Supplementary Fig. 9 | The comparison of soil carbon content between CMIP6 ESMs and NCSCDv2. a-h, Climatology of annual mean soil carbon pool in northern mid-high latitudes at pre-industrial era in CMIP6 ESMs **(a-g)**. The storage of soil organic carbon in permafrost region between 0-300cm depth from the Northern circumpolar soil carbon data version 2 (NCSCDv2)[5] **(h)**. The simulated permafrost extent in each ESM and boundary of continuous and discontinuous permafrost from the CCI-PF data[6] are superimposed in green and blue, respectively.

Supplementary Table 1 | CMIP6 ESMs used in this study

Model Name	Modeling Center (or Group)	References
ACCESS-ESM1-5	Commonwealth Scientific and Industrial Research Organisation	(7)
CanESM5	Canadian Centre for Climate Modelling and Analysis	(8)
CESM2	National Center for Atmospheric Research	(9)
CNRM-ESM2-1	National Centre for Meteorological Research	(10)
GFDL-ESM4	NOAA Geophysical Fluid Dynamics Laboratory	(11)
MIROC-ES2L	Japan Agency for Marine-Earth Science and Technology	(12)
NorESM2-LM	Norwegian Climate Centre	(13)
UKESM1-0-LL	Met Office Hadley Centre	(14)

Supplementary Table 2 | Description of land components in ESMs

Model Name	Land Surface Model	Soil layer/ depth (m)	Permafrost carbon	Nitrogen cycle	Fire	Dynamic vegetation
ACCESS-ESM1-5	CABLE	6/2.9	No	Yes	No	No
CanESM5	CLASS-CTEM	3/4.1	No	No	No	No
CESM2	CLM5	25/42.0	Yes	Yes	Yes	No
CNRM-ESM2-1	SURFEX	14/10.0	No	No	Yes	No
GFDL-ESM4	LM3.0	20/8.8	No	No	Yes	Yes
MIROC-ES2L	MATSIRO6.0/ VISIT-e	6/9.0	No	Yes	No	No
NorESM2-LM	CLM5	25/42.0	Yes	Yes	Yes	No
UKESM1-0-LL	JULES-ES-1.0	4/2.0	No	Yes	No	Yes

Supplementary Table 3 | The lag in global total land C stock

(Unit: Gt C)	$2\times CO_2$ (210 – 70)	$1\times CO_2$ (280)	At the end of exp. (335)
Global	358.0 ± 102.3	284.8 ± 64.2	111.8 ± 37.5
Tropic (30°S–30°N)	145.3 ± 60.7	90.0 ± 32.1	7.3 ± 15.0
Mid-high latitudes (Above 30°N)	201.1 ± 67.0	184.8 ± 56.0	99.5 ± 40.7

Uncertainties are expressed as the standard error.

Supplementary References

1. Kug, J. S. *et al.* Hysteresis of the intertropical convergence zone to CO_2 forcing. *Nat. Clim. Chang.* **12**, 47–53 (2022).
2. Lawrence, D. M. *et al.* The Community Land Model Version 5: Description of New Features, Benchmarking, and Impact of Forcing Uncertainty. *J. Adv. Model. Earth Syst.* **11**, 4245–4287 (2019).
3. Burke, E. J., Zhang, Y. & Krinner, G. Evaluating permafrost physics in the Coupled Model Intercomparison Project 6 (CMIP6) models and their sensitivity to climate change. *Cryosphere* **14**, 3155–3174 (2020).
4. Koven, C. *et al.* Multi-century dynamics of the climate and carbon cycle under both high and net negative emissions scenarios. *Earth Syst. Dyn.* **13**, 885–909 (2022).
5. Hugelius, G. *et al.* A new data set for estimating organic carbon storage to 3 m depth in soils of the northern circumpolar permafrost region. *Earth Syst. Sci. Data* **5**, 393–402 (2013).
6. Obu, J. *et al.* Northern Hemisphere permafrost map based on TTOP modelling for 2000–2016 at 1 km^2 scale. *Earth-Science Rev.* **193**, 299–316 (2019).
7. Ziehn, T. *et al.* The Australian Earth System Model: ACCESS-ESM1.5. *J. South. Hemisph. Earth Syst. Sci.* **70**, 193–214 (2020).
8. Swart, N. C. *et al.* The Canadian Earth System Model version 5 (CanESM5.0.3). *Geosci. Model Dev.* **12**, 4823–4873 (2019).
9. Danabasoglu, G. *et al.* The Community Earth System Model Version 2 (CESM2). *J. Adv. Model. Earth Syst.* **12**, e2019MS001916 (2020).
10. Séférian, R. *et al.* Evaluation of CNRM Earth System Model, CNRM-ESM2-1: Role of Earth System Processes in Present-Day and Future Climate. *J. Adv. Model. Earth Syst.* **11**, 4182–4227 (2019).

11. Dunne, J. P. *et al.* GFDL's ESM2 Global Coupled Climate–Carbon Earth System Models. Part I: Physical Formulation and Baseline Simulation Characteristics. *J. Clim.* **25**, 6646–6665 (2012).

12. Hajima, T. *et al.* Development of the MIROC-ES2L Earth system model and the evaluation of biogeochemical processes and feedbacks. *Geosci. Model Dev.* **13**, 2197–2244 (2020).

13. Tjiputra, J. F. *et al.* Evaluation of the carbon cycle components in the Norwegian Earth System Model (NorESM). *Geosci. Model Dev.* **6**, 301–325 (2013).

14. Sellar, A. A. *et al.* UKESM1: Description and Evaluation of the U.K. Earth System Model. *J. Adv. Model. Earth Syst.* **11**, 4513–4558 (2019).